Article Identifier
DOI: 10.22032/dbt.58725
URN: urn:nbn:de:gbv:ilm1-2023isc-118:3

60th ILMENAU SCIENTIFIC COLLOQUIUM
Technische Universität Ilmenau, 4 – 8 September 2023
URN: urn:nbn:de:gbv:ilm1-2023isc:1

INSIGHTS INTO THE WRITING PROCESS OF THE MASK-FREE NANOPRINTING FLUID FORCE MICROSCOPY TECHNOLOGY

Marcus Soter,[1] Gurunath Apte,[1,2] Dikshita Madkatte,[1] and Thi-Huong Nguyen[1,3*]

[1]Institute for Bioprocessing and Analytical Measurement Techniques (iba), 37308 Heilbad Heiligenstadt, Germany

[2]Institute of Nanotechnology (INT) and Karlsruhe Nano Micro Facility (KNMFi), Karlsruhe Institute of Technology, 76131 Karlsruhe, Germany

[3]Faculty of Mathematics and Natural Sciences, Technische Universität Ilmenau, 98694 Ilmenau, Germany

ABSTRACT

Platelets are activated immediately when contacting with non-physiological surfaces. Minimization of surface-induced platelet activation is important not only for platelet storage but also for other blood-contacting devices and implants. Chemical surface modification tunes the response of cells to contacting surfaces, but it requires a long process involving many regulatory challenges to transfer into a marketable product. Biophysical modification overcomes these limitations by modifying only the surface topography of already approved materials. The available large and random structures on platelet storage bags do not cause a significant impact on platelets because of their smallest size (only 1-3 µm) compared to other cells. We have recently demonstrated the feasibility of the mask-free nanoprint fluid force microscope (FluidFM) technology for writing dot-grid and hexanol structures. Here, we demonstrated that the technique allows the fabrication of nanostructures of varying features. Characteristics of nanostructures including height, width, and cross-line were analyzed and compared using atomic force microscopy imaging. Based on the results, we identified several technical issues, such as the printing direction and shape of structures that directly altered nanofeatures during printing. We confirmed that FluidFM is a powerful technique to precisely fabricate a variety of desired nanostructures for the development of platelet/blood-contacting devices if technical issues during printing are well controlled.

1. INTRODUCTION

Platelet products are collected directly from human blood and stored in plastic bags before transfusion. It was reported that around 1300 liters of platelet concentrate are daily transfused in Germany alone,[1] and 118.54 million blood donations are annually collected globally every year.[2] In the US alone, approx. 30,000 potentially preventable deaths per year after traumatic injury due to severe bleeding.[3] Platelet transfusion demand increased because of the increase in intensive chemotherapy and hematopoietic stem cell transplantation as well as highly invasive surgical operations in several specific areas, such as cardiovascular surgery. However, above 1/2 of the US patients suffer from >1-hour delay before treatment in a level 1 trauma center,

and thus, lacks access to hemostatic resuscitation in the crucial minutes after injury.[3] The problem is derived from the difficulties during the management of platelet storage. Smaller hospitals generally cannot stock platelets, while in larger centers, platelet concentrates are mostly used for hematology-oncology patients only.[3]

Platelets are fragments of cells that are developed from mature cell megakaryocytes in the bone marrow.[4] A single megakaryocyte can produce >1,000 platelets that are stored in the spleen and blood circulation. A healthy adult contains 150,000-450,000 platelets/µL blood. Platelets are the smallest blood cells (size between 1 and 3 µm). They do not have a nucleus, and thus, are extremely sensitive. They tend to activate immediately after a short time contacting with any artificial surfaces.[5-6] Platelet concentrates are normally pooled from 4 to 6 donor units to obtain an adult dose of at least 240 x 10^9 platelets.[7] Current technologies allow the storage of platelets at room temperature for only 72 hours (WHO).[7] The first problem with longer storage is the drop in pH because platelet produces a considerable amount of lactic acid and CO_2 when metabolizing glucose and consuming O_2. A low pH ultimately leads to platelet storage lesions such as platelet activation, the exhibition of apoptotic markers, and low recoveries.[9] The second problem with longer storage is the increased risk of bacterial contamination.[10-13] WHO reported that bacterial contamination affects about 1% of pooled units.[7] The short shelf life together with unpredictable demand results in platelet inventory management problems as manifested by high rates of outdating (up to 23%),[14] leading to a higher cost of platelets than other blood products such as fresh-frozen plasma or red blood cells.[15] The short storage period limits platelet transfusion in many emergency stations. According to the Blood Product Utilization Guidelines (The University of Mississippi, Medical Center), platelet transfusions may be limited only to patients with life-threatening bleeding if necessary, to preserve a limited platelet inventory.[16] During blood product shortage, the platelet transfusion thresholds will be lowered,[16] that may cause higher risks for patients. If old platelets are infused in patients, a decrease in transfusion efficacy and an increase in adverse events such as transfusion-associated sepsis and immune-mediated events occur, especially, in hematology, oncology, and post-cardiac surgery patients.[11] Less than one percent of the total blood can be isolated as platelets. These problems together with the highly sensitive characteristics of platelets lead to extreme difficulties during storage management. Stored platelets after collection may become deactivated or dysfunctional towards the end of the storage time.[17] As a consequence, the total cost of platelet transfusions in a US hospital inpatient setting was raised to 1360$ per platelet unit.[17] Thus, an extension of the shelf life for platelet storage has both positive financial and inventory management outcomes.

Regarding platelet storage improvement, an important effort to introduce microtextures either on one or both sides of the bags has been developed to prevent the inside faces from sticking during heat sterilization or processing.[18] However, these microstructures exhibit several limitations such as the enhancement of platelet adhesion and bacterial growth.[19-20] Adherent platelets immediately activate and transform into filopodia and lamellipodia,[21] causing several bioactive chemicals to be released, which may lead to platelet aggregation or breakdown in bags. This further enhances the drop of pH in the platelet bag.[21] A similar or even more complicated thrombogenic mechanism can occur on many medical devices such as transfusion apparatus and implants.[22] It has been reported that platelet adhesion/activation on an implant obstructs the functionality of the materials and causes blood vessel narrowing.[23-24] Consequently, patients who receive implants are often given high doses of anticoagulants.[25] Venous catheters, vascular grafts, stents, and heart valves have been previously associated with thrombotic complications, resulting in failures, body rejections, or even stroke and heart attacks.[26] Thus, the material-blood interaction is critical in determining the body's acceptance of the implants.[27] As the contact adherence of platelets on biomaterials is the first step in the formation of a thrombus,[28] minimizations of surface-induced platelet activation play a crucial role in the development of ideal blood storage bags and overcoming current limitations in

platelet-contacting devices. For decades, the improvement of blood-contacting materials has still been suffering from major challenges.[29]

While microstructures have only a minor effect on platelets, nanostructures that are placed directly underneath the platelets can govern cellular response. However, currently, available technologies for the fabrication of nanostructured surfaces using commercially available synthetic as well as bio-based mono- and polymers are limited. Even though two-photon polymerization (2PP) allows to print structures down to 100 nm,[30-31] the technique is time-consuming, complex, inefficient for fabrication of a large sample size, and only works with photo-polymerizable materials. The mask-free FluidFM-based atomic force microscopy (AFM) technology is a versatile method for generating functional and topographical features ranging from synthetic[31,32] to biological materials.[33] The use of the FluidFM enables the cost- and time-efficient production of almost limitless prototype structures. Previously, we have demonstrated the feasibility of the FluiFM in printing dot-grid and hexagonal nanostructures using a commercial hybrid acrylate-based UV curable Loctite AA3491 (Henkel).[32] These structures caused a reduction of surface stiffness and inhibited platelet adhesion and activation. In this study, we demonstrated that FluiFM allows to fabricate nanostructured surfaces of varying features. By characterizing the height, width, and transverse line, of the printed nanostructures, and comparing them, we identify that printing direction, shapes of structures, and tip-effect directly altered nanofeatures during printing. Our results indicate that FluidFM is a powerful fabrication technique to produce a variety of desired nanostructures for the development of platelet/blood-contacting devices if the printing parameters and technical issues are well controlled.

2. METHODS

Ethics

The use of blood obtained from healthy volunteers was approved by the ethics board of Thüringen, Germany.

FluidFM based printing

The structures were printed using a Nanowizard 4 setup (JPK, Berlin, Germany) with a FluidFM add-on (Cytosurge, Opfikon, Switzerland), placed under an acoustic hood, and mounted on an active vibration isolation system (Micro 40, Halcyconics, Germany) to mitigate the effect of external vibrations. The cantilever was observed and moved to the desired spots using an inverted microscope (Axio Observer Zeiss, Jena, Germany). Before printing, the structures were first designed using Inkscape (version 0.17), an open-source vector-based graphics application that enables users to create and modify the desired pattern to an exportable scaled vector graphic file (SVG). This pre-designed structure was imported into the AFM control program JPK Nanowizard4. As print material, the commercially available Loctite AA3491 (Henkel, Düsseldorf, Germany), made up of a combination of different methacrylate esters that polymerize when exposed to UV light was filled in the reservoir of microchannel cantilever, was used. The Loctite AA3491 is composed of monomers from isobornyl acrylate, 2-hydroxyethyl methacrylate, acrylic acid, and hydroxypropyl acrylate.[34] Before each printing cycle, a nanopipette with an aperture of 300 nm and a nominal spring constant of 2 N/m (Cytosurge, Opfikon, Switzerland) was calibrated using the contact-free thermal noise method before being approached to the surface. In manipulation mode, the structures were printed on a glass coverslip (Plano GmbH, Wetzlar, Germany) of 24 mm which was pre-cleaned with 80% Ethanol under 30 min sonication. The printing was done in an area of 100 × 100 µm by upholding a steady positive pressure of 20 mbar, set point of 20 nN, and writing speed of

12 µm/s. For polymerization, the samples were cured after printing using a UV lamp at 365 nm for 5 min.

Characterization of printed structures using atomic force microscopy (AFM)

In order to determine the dimension of the printed nanostructures such as height, width, and interspaces as well as the changes in structures during printing, we imaged the samples using AFM. As AFM provides an atomic resolution, detailed changes caused by printing directions or raised by specifically designed structures could be visualized. The AFM topological images were obtained by scanning surfaces in contact mode. All the samples were imaged using a cantilever from Bruker (MLCT-Probe A) with a nominal spring constant value of 0.07 N/m at a line rate of 0.3 Hz and a resolution of 512 × 512 pixels and a scan size of 100 x 100 µm. Using JPK software (JPK Nanowizard4) for analysis, the line profiles of the features were accomplished by selecting the image cross-section option to determine the size of each printed feature. To compute the mean and standard deviation, the height and width of at least 25 features were measured.

Platelets extraction from blood

Blood was drawn into a 10 mL blood collecting tube containing 1.5 mL acid-citrate dextrose ACD-A (BD-Vacutainer, Berlin, Germany) from healthy human donors who had not consumed any drugs in the previous two weeks. The blood tube was sealed with parafilm, inclined at an angle of 45°, and rested at room temperature for 15 min before centrifugation. Firstly, blood was centrifuged at 120 g for 20 min at room temperature to separate platelet-rich plasma (PRP) from the blood. Further, platelet isolation from PRP was accomplished by centrifuging at 650g for 7 minutes in a buffer containing 11% ACD-A (Fresenius Kabi, Germany) and 2.5 U/mL Apyrase (grade IV SIGMA, Munich, Germany). The platelet pellet was resuspended in 1 mL of suspension buffer at pH 6.3, consisting of 137 mM NaCl, 2.7 mM KCl, 11.9 mM $NaHCO_3$, 0.4 mM Na_2HPO_4, and 2.5 U/mL Hirudin. Following that, an additional 4 mL of suspension buffer was added, and the platelets were incubated at 37°C for 15 min. The suspension was then centrifuged again for 7 minutes at 650g. Following a second resuspension of platelet pellets in 2 mL of suspension buffer, platelet counting was carried out using a blood counter (pocH-100i, SYMEX, Germany). In the suspension buffer, the platelet concentration was further adjusted to 30,000/µL for sample stabilization and rested at 37°C for 45 min before use.

Platelet adhesion on storage bags

The platelet adhesion on a plastic bag was performed to get an insight into platelet activation on a commercially available storage bag (Terumopenpol, Thiruvananthapuram, India). A Storage bag pieces of 1 x1 cm were cut from the bag and cleaned under UV ozone for 30 min. After that, platelets of 30,000/µL were added to bag pieces and incubated for 1 hour After rinsing with phosphate buffer silane (PBS) to eliminate any remaining unbound platelets, 4% Paraformaldehyde (PFA) was added to fix the platelets. After fixation, the platelets were stained for 1 hour with an anti-CD42a FITC antibody (Dianova GmbH, Hamburg, Germany) at a final concentration of 1 µL/mL of platelet solution to quantify the adherent platelets on the surface. The sample was then washed twice with PBS to remove the unbound dye before examining by the confocal laser scanning microscopy Zeiss LSM710 (Carl Zeiss, Gottingen, Germany) at room temperature in the dark. The red fluorescent signal was acquired at an excitation/emission wavelength λ = 580/599 nm using a 63x objective. Also, a T80/R20 beam splitter was used for taking images to perform confocal reflection microscopy on the patterns.

3. RESULTS AND DISCUSSION

3.1. Dissimilar response of platelets on micro- and nanostructures

To identify the dissimilar effect of micro and nanostructures on the response of platelets, we compared the response of platelets on these structures. A commercially available bag that contains microstructures was tested. Platelets were incubated on this bag and stained P-selectin using CD42a FITC antibody for imaging with a confocal microscope. A high density of platelets adhered to the bag, both on microstructures and outside the structured surfaces (**Figure 1A-C**). A similar observation was also reported in the literature.[19-20] This clearly shows no effect of large structures on the inhibition of surface-induced platelet adhesion. As any adhered platelets will be activated quickly,[21] they release from their intracellular granules namely dense granules, multiple bioactive molecules such as adenosine diphosphate (ADP), adenosine triphosphate (ATP), guanosine 5′-[β-thio]diphosphate (GDP), 5-hydroxytryptamine (5-HT) and PF4. These bioactive molecules further trigger platelet adhesion by signaling positive feedback and cause activation of integrin αIIbβ3 and fibrin which lead to the formation of a thrombus or a platelet plug. This can cause aggregation/degradation and alter the storage buffer over time.[9, 33] Bacterial film formation on this type of bag has been also reported.[19-20] Thus, the commercially available structured surface does not inhibit platelet adhesion/activation or improve platelet storage.

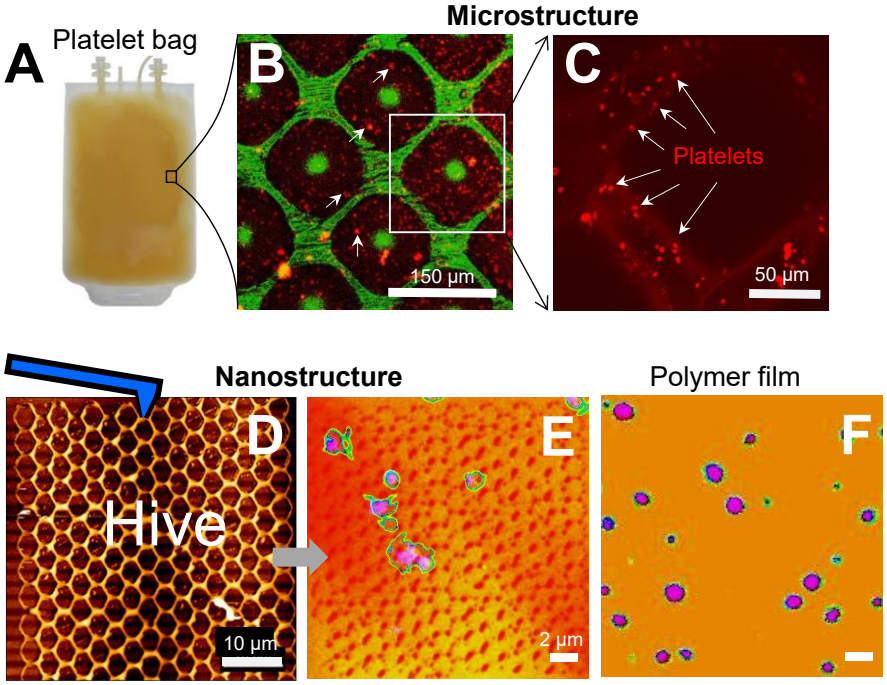

Figure 1. Distinct adhesion phenomenon of platelets on micro- and nanostructures. (**A**) Platelet concentrates are collected from healthy blood donors and stored in commercially available structured plastic bags before transfusing to life-threatening bleeding patients. (**B**) Platelets (arrows) adhered and aggregated on nonstructured surfaces. (**C**) The enlargement shows multiple platelets adhered to the structured surfaces (arrows). (**D**) Nanostructures with hive (=hexagonal) features printed with FluidFM strongly reduce platelet adhesion (**E**) as compared with (**F**) nonstructured polymer film of the same material (adapted from[32]).

We have previously proven that the commercial hybrid acrylate-based UV curable Loctite AA3491 (Henkel) allowed the printing of several types of nanostructures such as hive (=hexagonal) features (**Figure 1 D**).[32, 34] These nanostructures strongly reduce platelet adhesion as shown by a low density of platelets (**Figure 1E**) compared with a high density of cells on

the nonstructured polymer film (**Figure 1F**). Our findings demonstrated the important role of nanotextures in the inhibition of platelet-surface adhesion and activation. However, we have so far only been successful in printing dot-grid and hive structures. In the next section, we report challenges in the fabrication of nanostructures with multiple features.

3.2. Design for mask-free nanoprinting with fluid force microscope (FluiFM)

To print other types of nanostructures, we used here FluidFM and also a commercial hybrid acrylate-based UV curable Loctite AA3491 (Henkel) ink. The ink was injected in a microchannel probe connected with a tip aperture of ~300 nm. By applying a pressure of 20 mbar, the ink was pushed through the aperture to generate nanostructures (**Figure 2A**). The structures were cured under a UV source at 365 nm wavelength. **Figure 2B**). As previously observed hexagonal (=hive) structures show effective platelet inhibition compared to dot-grid structures,[32] here we printed other structures with platelet-like shapes including grid, circle, triangle, and Pacman-like features. We hypothesize that the continuous and symmetrical features are favorable surfaces for platelets because they generate a homogeneous and gentle matrix underneath them and thus, reduce platelet adhesion and activation. Importantly, by printing these designed structures, we aim to understand the feasibility of FluidFM in printing various complexities of structures. Within these designed structures, the FluidFM cantilever must move in a linear and non-linear direction and the contact angle of the tip is changed during printing. This effect has not been thoroughly understood in the literature yet.

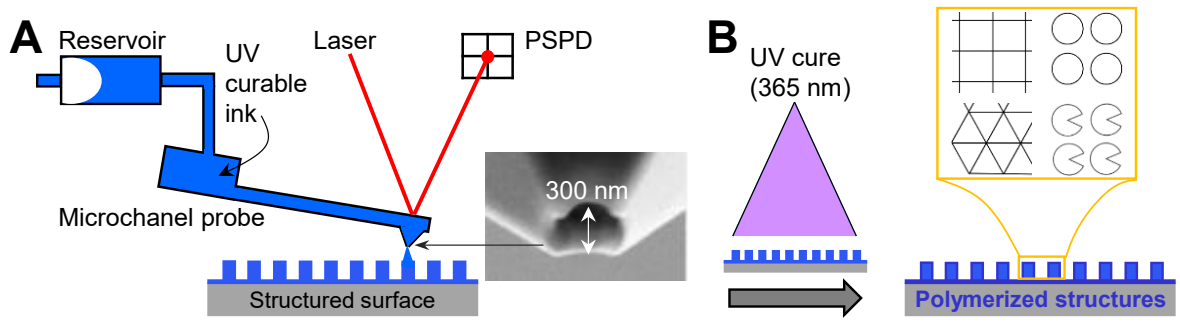

Figure 2. **The scheme shows the principle for the fabrication of nanostructured surfaces using FluidFM**. (**A**) FluidFM prints structures using UV-curable ink injected in a microchannel probe (blue) with a tip aperture of ~300 nm. By applying a force to the cantilever together with pressure through the reservoir, a pattern of designed structures will be printed in a force-manipulation mode. (**B**) The structured surface is formed after UV curing at a wavelength of 365 nm. Platelet-like features including grid, circle, triangle, and Pacman-like structures are printed.

3.3. Fabrication of structured surfaces of different features

To fabricate the structures, ink was loaded into the microchannel probe connected to a cantilever with a tip aperture of ~300 nm. The designed structures were loaded into the JPK software for printing under manipulation mode. By applying pressure, the ink from the microchannel probe was pushed through the cantilever aperture for printing the patterns. We have successfully printed four types of structures including grid, circle, triangle, and Pacman-like as viewed by light microscopy images (**Figure 3A**). AFM images allow determination of the height and width of the structures (**Figure 3A**) *via* analysis of line profiles. We compared those parameters among the printed structures (**Figure 3B, white lines**). In Figure 3C, the corresponding height profiles are shown. Data collected from different line profiles are presented as box plots for height (**Figure 3D**) and width (**Fig. 3E**). For all measurements, a relatively low variation of measured height/width was observed, indicating a good reproducibility of the FluidFM in fabricating micro-/nanostructures. However, both height

(**Figure 3D**) and width (**Figure 3E**) changed depending on the feature of the designed structures. Additionally, the height, as well as the width in individual structures, was not uniform. For the grid, the structures are rather uniform (226.0 ± 21.2 nm) (**Figure 3D**). The circles show two distinct heights (point-1 and point-2, **Figure 3B-D**) in which point-2 displays the merging of two close circles. Triangle lines are higher than the grid, circle-1, and Pacman height. The Pacman-like structures also show two different heights (point-1 and point-2, **Figure 3B, C, E**). Among these structures, the heights vary up to 400 nm, except for the merging of the circles at point-2. The widths at these analysis points also varied depending on the features of structures (**Figure 3E**). Our results indicate that the printing direction caused by the features of the desired structures plays an important role in the resulting dimension of the structures.

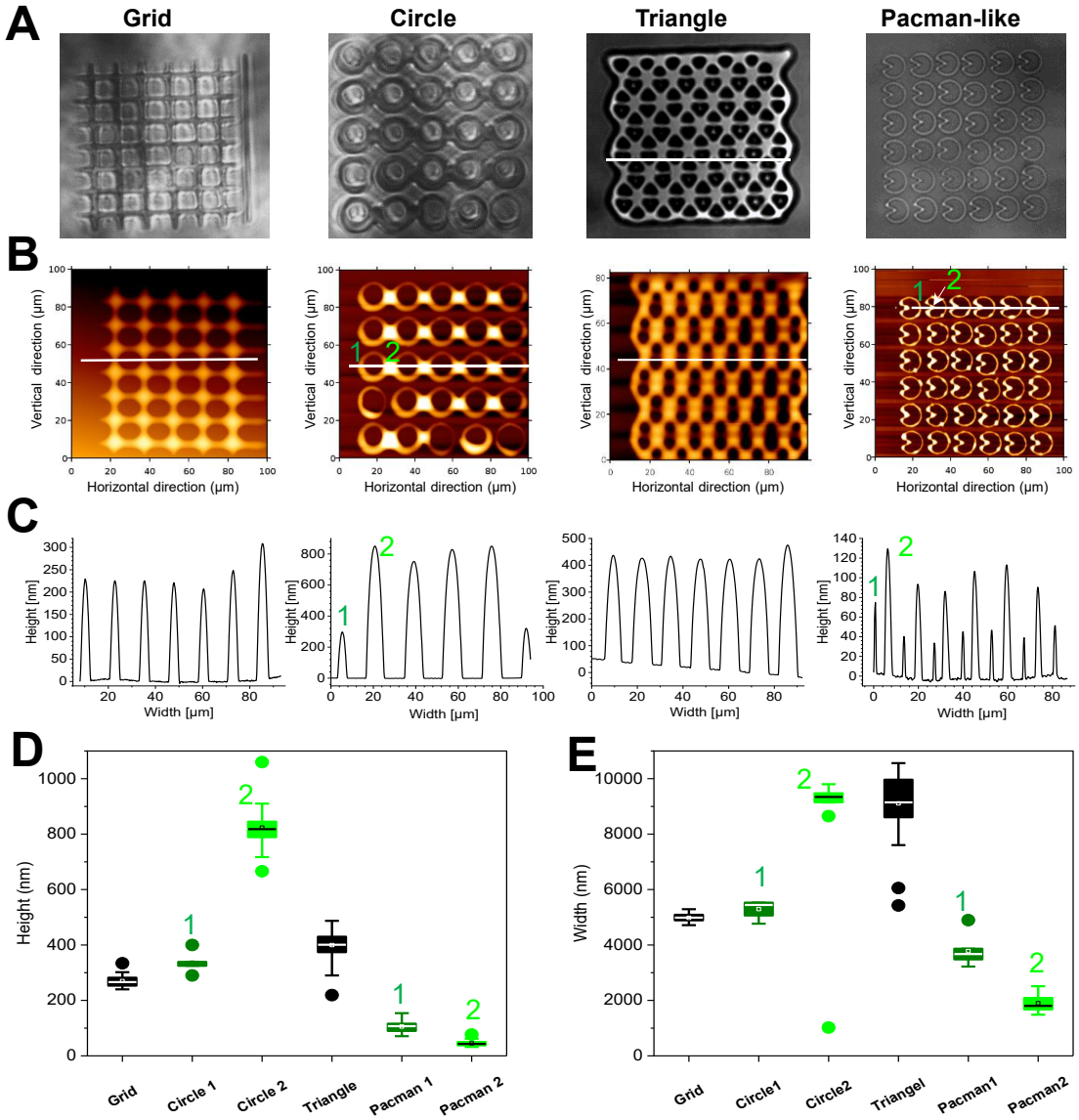

Figure 3. **Fabrication of nanostructures of different features by FluidFM**. (**A**) Light microscopy images show four platelet-like features including grid, circle, triangle, and Pacman-like structure. (**B**) AFM images and (**C**) Height changes at the corresponding line profiles were taken horizontally on the structures. (**D**) Height and (**E**) width values collected from different line profiles differed among printed structures. Circle and Pacman-like showed two distinct heights point-1 and 2 (**green, B-D**).

3.4. Insights into nanoprinting process

To gain insights into the process while nanoprinting, we enlarged the structures and compared the width, height, and also cross-section for each type of feature by analyzing AFM line profiles

(Fehler! Verweisquelle konnte nicht gefunden werden.). Figure 4A shows 3-D (top panels) and 2-D (low panels) images with changes of printing lines depending on printing direction (white arrows) and features of structures. To understand the effect of printing direction, we compared the structural height and width in the vertical or horizontal direction (Fehler! Verweisquelle konnte nicht gefunden werden.**, blue and green lines, respectively**). To gain insight into the layer-by-layer printing procedure, we analyzed the cross-section at the knots (Fehler! Verweisquelle konnte nicht gefunden werden.**A, C, violet lines**) where up to three printing lines were superimposed.

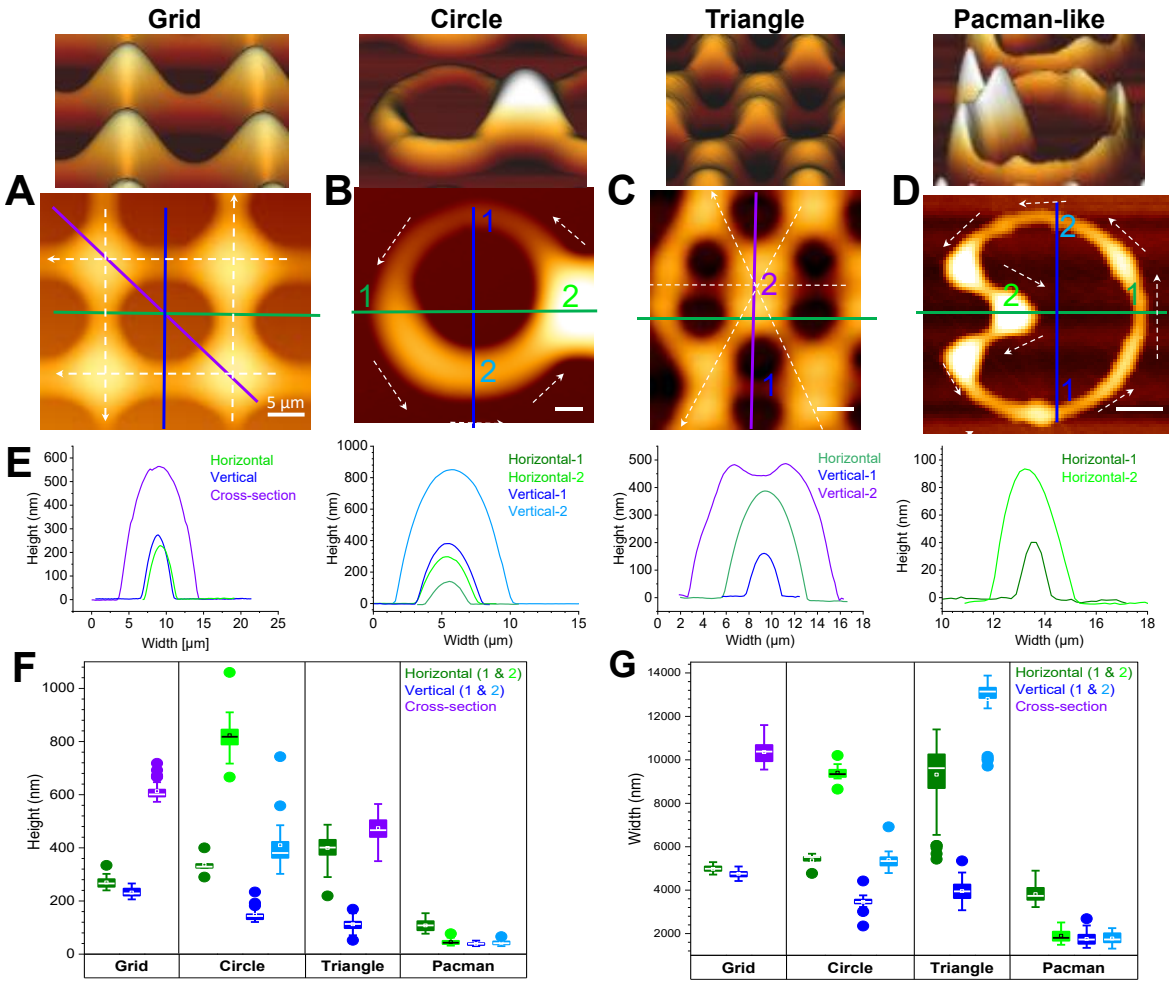

Figure 4. **Effect of printing direction and features of structures on printing results.** (**A**) 3-D (top panels) and 2-D (lower panels) images taken by AFM show the changes in printing size depending on the printing direction (white arrows) and the features of structures. Analysis of line profiles of the structures measured horizontally (green) or vertically (blue), and at the knots where two (**A, violet**) or three (**C, violet**) printing lines are superimposed. The unequal ink distribution while printing (**B**) Circles and (**D**) Pacman-like structures were compared by analysis of image line profiles. (**E**) Comparison of line profiles at different positions for each structure showed dissimilar heights and widths. (**F**) Height and (**G**) Width from all printed structures at different analysis positions showed significant changes in structures**.**

For grid structure, printing in the vertical direction resulted in a lower height (220 ± 16 nm) than in the horizontal direction (266 ± 21 nm). A similar effect for the width, 4759 ± 162 nm in the vertical direction and 4985 ± 131 nm in the horizontal direction were observed (**Table 1**). The results indicate that the writing direction caused changes in the dimension of the designed structures. This effect could also be seen in the triangular shape. The height of single lines in the vertical direction of the triangles is approximately the same as that of the grid. However,

much larger width (9616 ± 1362 nm) and higher height (401 ± 47 nm) were seen in the horizontal direction which can be explained by the merging of two printing lines. The influence of the writing direction becomes more interesting when analyzing the circular structures. Within a circle, both height and width at point-1 differ from those at point-2. At point-2, a high amount of ink was transferred to the substrate, resulting in merged structures of two close circles. Therefore, the height and width at point-2 in the horizontal direction display the value for the merged structures. The shape of the cantilever also likely played a role. Probably, the non-flat, asymmetric end of the tip aperture led to unequal output of ink when the cantilever printed the different angles. This resulted in a highly different amount of ink (either less or more) distributed to the substrate, leading to a large variation within a circle (818 nm *vs* 329 nm in height and 5528 nm *vs* 3943 nm in width corresponding to measurements at point-2 and point-1). The Pacman-like structures are a combination of line and circular shapes. In comparison to circles or lines only, the height and width of Pacman-like structures are reduced. At the circular part, the height is approx. 40 ± 10 nm which is only about 10% of the height of the circular-shaped structures without lines. Besides, the line part has a height of 107 ± 17 nm and width of 3737 ± 379 nm which is lower than those for lines only in grid or triangle structures.

Table 1. Width and height depend on printing structures and measuring points.

Structure		Height (nm)	Width (nm)
Grid	Horizontal	226.0 ± 21.2	4985.0 ± 131.5
	Vertical	228.5 ± 15.7	4759.0 ± 162.4
	Cross-Section	601.0 ± 27.9	10380.0 ± 529.7
Circle	Horizontal-1	329.0 ± 35.7	5528.0 ± 317.2
	Horizontal-2	818.0 ± 80.9	3943.5 ± 327.4
	Vertical-1	143.5 ± 24.7	3457.0 ± 332.4
	Vertical-2	380.5 ± 86.7	5339.0 ± 407.2
Triangle	Horizontal	401.0 ± 46.5	9616.0 ± 1362.2
	Vertical-1	113.5 ± 24.0	3942.0 ± 489.0
	Vertical-2	466.5 ± 41.7	13145.0 ± 1076.5
Pacman	Horizontal-1	107.0 ± 17.2	3737.0 ± 379.3
	Horizontal-2	43.0 ± 9.8	1803.0 ± 271.8
	Vertical-1	39.0 ± 5.1	1725.0 ± 282.2
	Vertical-2	41.0 ± 8.0	1728.0 ± 240.9

Our results indicate the influence of the tip geometry and printing direction while writing structures of different geometries. As shown in Figure 2 (inset), the geometry of the probe is not equal in all directions. Due to the shape, the amount and output of ink in the different directions is influenced. The tip effect had little impact on the grid structure, but it had a significant impact on the circular-shaped structures, resulting in printed features that were dissimilar from the desired structures. In contrast to lines, the circular structures, displayed all directions at once while all the angles of the probes were used in order to write a circle. It can be seen that the amount of ink distributed to the substrate was guided by the movement direction of the FluidFM probe. Our observation is in line with a previous study showing the influence of the printing direction on the linewidth in which a direction-dependent difference in the height increased up to 10-fold.[35] However, this study only reported the impact on printing lines. The height of the printed lines was only between 10 - 20 nm. In our work, a significantly higher height and width can be shown even though the same Loctite ink was used. This difference can be due to the printing parameter used such as printing speed and tip contact time. We have previously found that printing speed and contact time have a major effect on the size of the

structures whereas other parameters such as setpoint and applied pressure do not cause a significant change (**Table**).[32]

Table 2. Effect of setting parameters during FluiFM printing.[32]

Printing parameters	Effect on the width of structures	Range
Contact time	strong	≤ 20 s
Writing velocity	strong	≤ 2.2 µm/s
Setpoint	weak	≤ 20 nN
Pressure	weak	≤ 70 mbar

Besides this, it must be taken into consideration that while printing the lines in manipulation mode, the FluidFM probe moved in one x (or y)-direction only while the y (or x)-direction was fixed. When printing circles, the tip moved with small steps in both x and y-directions to fulfill a circular shape. These different processes between printing lines and circles can be recognized better when combining them in the Pacman-like structure that is a combination of both lines and circles. The amount of ink applied in the circular part was much less than for circles only. Here, it seems that the tip contacted the substrate during printing at both linear and circular parts.

Besides narrow width, the higher height of the structures can prevent the platelets from contacting with the substrate, and thus, reduce platelet activation. In principle, the height can be increased by layer-by-layer deposition. In our designed grid and triangle structure, the knots (=crossed areas) are composed of superimposed writing lines that can be considered as a double layer. In comparison to printing one line, the crossed area where two times ink was applied, shows a higher height (601 ± 28 nm) compared to the combined/sum height of both vertical (228 ± 16 nm) and horizontal (266 ± 21 nm) lines when printed separately. For triangles, in the cross knot area, it was three times printed but the height of the 3-fold single line print was not seen. Here, the height was even reduced (about 220 nm, **Fig. 5**) compared to the double height of two single lines. Interestingly, the line profile at the cross area in the triangles show a valley (approx. 55 nm) on the top of the structures (

). The first two application of ink likely leads to a rise in the height but the third one was not successful. Instead of adding ink, the tip took away some nanodrop of ink, leaving a groove at the top of the structures, leading to a reduction in height. It seems that the previously printed ink layer was at the starting phase of drying. Under an applied force, the tip indented the already partially dried structures, leaving a depth valley. Approaching the tip to the intermediate soft-hard interface, the open apertures of the cantilever seemed to be 'closed' by the partially dried flexible material. This resulted in no ink being transferred to the post-printed structures. To prevent this, the optimal ink viscosity and the time lag between the printing layers should be precisely adjusted. Furthermore, the volume of the ink required to deposit on each additional layer may differ and needs more optimization. Probably, when the

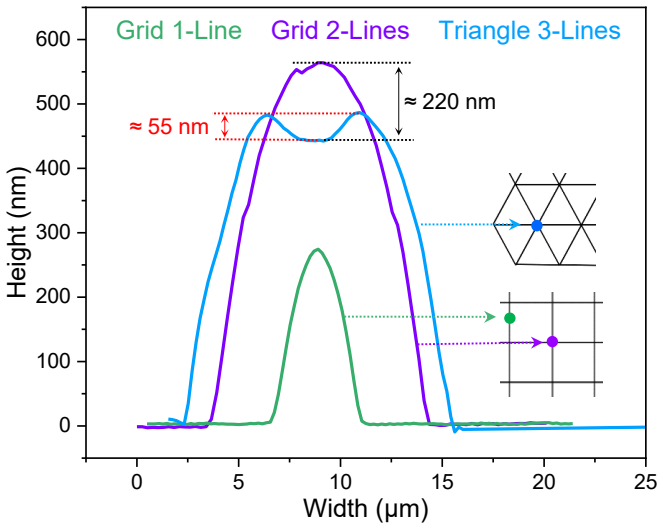

Figure 5. Differentiation between the height occurred by printing one (grid, green), two (grid, purple) and three (triangle, blue) layers.

structure become thicker by multiple additional layers, a higher ink volume is required to cover the whole surface of the post-printed structures.

In comparison to de Souza et al. who showed an increase in height by printing two layers,[35] we were also able to demonstrate an add-up of 2 layers while printing. The authors reported an increased height of the second layer of only 20% whereas we were able to show an increased height of the second layer up to 50% (**Fig. 5**). We postulate that due to our low printing speed (12 µm/s) compared with the faster printing (50-200 µm/s) in the study of Souza et al., the contact time between ink and substrate as well as between ink and ink was increased, leading to an enhanced adhesion among the old, newly added ink and the substrate.

4. CONCLUSION

We demonstrated that FluidFM allows to fabricate nanostructures of different features. Characteristics of structured surfaces including height, width, and cross/knots varied depending on the printing direction and the features of the designed structures. FluidFM printed precisely simple and straight structures but unequal height and width of the structures were observed when printing circles, triangles, and Pacman-like shapes. We explained the causes of nonhomogeneous structures and suggested a solution to overcome the identified technical issues caused by printing direction and complex shapes. In comparison with previous studies, we could produce structures of higher height utilizing a layer-by-layer platform. We confirmed that FluidFM is a powerful technique to precisely fabricate a variety of desired nanostructures for the development of platelet/blood-contacting devices. To fabricate optimized micro/nanostructures, numerous technical issues during printing should be controlled.

REFERENCES

1. Vit, G.; Klüter, H.; Wuchter, P., Platelet storage and functional integrity. *Journal of Laboratory Medicine* **2020,** *44*, 285-293.
2. WHO, Blood safety and availability. **26 May 2022**.
3. Cap, A. P.; Spinella, P. C., Just chill-it's worth it! *Transfusion* **2017,** *57* (12), 2817-2820.
4. Mcdonald, T. P., The regulation of megakaryocyte and platelet production. *The International Journal of Cell Cloning* **1989,** *7*, 139-155.
5. Bui, V. C.; Medvedev, N.; Apte, G.; Chen, L. Y.; Denker, C.; Greinacher, A.; Nguyen, T. H., Response of Human Blood Platelets on Nanoscale Groove Patterns: Implications for Platelet Storage. *ACS Applied Nano Materials* **2020,** *3*, 6996-7004.
6. Nguyen, T. H.; Palankar, R.; Bui, V. C.; Medvedev, N.; Greinacher, A.; Delcea, M., Rupture Forces among Human Blood Platelets at different Degrees of Activation. *Sci Rep* **2016,** *6*, 25402.
7. Czich, S.; Wloka, T.; Rothe, H.; Rost, J.; Penzold, F.; Kleinsteuber, M.; Gottschaldt, M.; Schubert, U. S.; Liefeith, K., Two-Photon Polymerized Poly(2-Ethyl-2-Oxazoline) Hydrogel 3D Microstructures with Tunable Mechanical Properties for Tissue Engineering. *Molecules* **2020,** *25* (21).
8. Kazuhiro Nagai, H. N., Yoshito Koga, Hiroshi Harada, Chiaki Yakushiji, Eiji Kino, Motoko Tokunaga, Hisatoki Yamaoka, Yasushi Miyazaki, The Usefulness of Improved, Newly Developed Polyolefin Container of Platelet, PO-100, with Higher Oxygen Permeability and Content. *Blood* **2018,** *132 (Supplement 1) : 1261*.
9. Dekkers, D. W. C.; De Cuyper, I. M.; Van Der Meer, P. F.; Verhoeven, A. J.; De Korte, D., Influence of pH on stored human platelets. *Transfusion* **2007,** *47*, 1889-1895.

10. Sahler, J.; Grimshaw, K.; Spinelli, S. L.; Refaai, M. A.; Phipps, R. P.; Blumberg, N., Platelet storage and transfusions: New concerns associated with an old therapy. *Drug Discovery Today: Disease Mechanisms* **2011,** *8*, e9-e14.
11. Aubron, C.; Flint, A. W. J.; Ozier, Y.; McQuilten, Z., Platelet storage duration and its clinical and transfusion outcomes: A systematic review. *Critical Care* **2018,** *22*, 185.
12. Levy, J. H.; Neal, M. D.; Herman, J. H., Bacterial contamination of platelets for transfusion: strategies for prevention. *Critical Care* **2018,** *22*, 1-8.
13. Arman, M.; Krauel, K.; Tilley, D. O.; Weber, C.; Cox, D.; Greinacher, A.; Kerrigan, S. W.; Watson, S. P., Amplification of bacteria-induced platelet activation is triggered by FcgammaRIIA, integrin alphaIIbbeta3, and platelet factor 4. *Blood* **2014,** *123* (20), 3166-74.
14. Flint, A. W.; McQuilten, Z. K.; Irwin, G.; Rushford, K.; Haysom, H. E.; Wood, E. M., Is Platelet Expiring Out of Date? A Systematic Review. *Transfus Med Rev* **2020,** *34* (1), 42-50.
15. Toner, R. W.; Pizzi, L.; Leas, B.; Ballas, S. K.; Quigley, A.; Goldfarb, N. I., Costs to hospitals of acquiring and processing blood in the US: a survey of hospital-based blood banks and transfusion services. *Appl Health Econ Health Policy* **2011,** *9* (1), 29-37.
16. The University of Mississippi, M. c., Blood Product Utilization Guidelines
17. Hofmann, A.; Ozawa, S.; Shander, A., Activity-based cost of platelet transfusions in medical and surgical inpatients at a US hospital. *Vox Sang* **2021,** *116* (9), 998-1004.
18. Prowse, C. V.; de Korte, D.; Hess, J. R.; van der Meer, P. F., Commercially available blood storage containers. *Vox Sanguinis* **2014,** *106*, 1-13.
19. Hadjesfandiari, N.; Schubert, P.; Fallah Toosi, S.; Chen, Z.; Culibrk, B.; Ramirez-Arcos, S.; Devine, D. V.; Brooks, D. E., Effect of texture of platelet bags on bacterial and platelet adhesion. *Transfusion* **2016,** *56* (11), 2808-2818.
20. Hadjesfandiari, N.; Weinhart, M.; Kizhakkedathu, J. N.; Haag, R.; Brooks, D. E., Development of Antifouling and Bactericidal Coatings for Platelet Storage Bags Using Dopamine Chemistry. *Advanced Healthcare Materials* **2018,** *7*, 1700839.
21. Jackson, S. P., The growing complexity of platelet aggregation. *Blood* **2007,** *109*, 5087-5095.
22. Weber, M.; Steinle, H.; Golombek, S.; Hann, L.; Schlensak, C.; Wendel, H. P.; Avci-Adali, M., Blood-Contacting Biomaterials: In Vitro Evaluation of the Hemocompatibility. *Frontiers in Bioengineering and Biotechnology* **2018,** *6*, 99.
23. Reviakine, I.; Jung, F.; Braune, S.; Brash, J. L.; Latour, R.; Gorbet, M.; van Oeveren, W., Stirred, shaken, or stagnant: What goes on at the blood–biomaterial interface. *Blood Reviews* **2017,** *31*, 11-21.
24. Gibbins, J. M., Platelet adhesion signalling and the regulation of thrombus formation. *Journal of Cell Science* **2004,** *117*, 3415-3425.
25. Baser, O.; Supina, D.; Sengupta, N.; Li, W., Anticoagulation bridging therapy patterns in patients undergoing total hip or total knee replacement in a us health plan: Real-world observations and implications. *American Health and Drug Benefits* **2011,** *4*, 240.
26. Jaffer, I. H.; Fredenburgh, J. C.; Hirsh, J.; Weitz, J. I., Medical device-induced thrombosis: What causes it and how can we prevent it? *Journal of Thrombosis and Haemostasis* **2015,** *13*, S72-S81.
27. Park, J. B.; Lakes, R. S., Soft Tissue Replacement — II: Blood Interfacing Implants. *Biomaterials* **2007**, 331-367.
28. Baumgartner, H. R.; Muggli, R.; Tschopp, T. B.; Turitto, V. T., Platelet adhesion, release and aggregation in flowing blood: effects of surface properties and platelet function. *Thromb Haemost* **1976,** *35* (1), 124-38.
29. Ratner, B. D., The catastrophe revisited: Blood compatibility in the 21st Century. *Biomaterials* **2007,** *28*, 5144-5147.

30. Park, S.; Kim, D.; Park, S.; Kim, S.; Lee, D.; Kim, W.; Kim, J., Nanopatterned Scaffolds for Neural Tissue Engineering and Regenerative Medicine. *Advances in Experimental Medicine and Biology* **2018,** *1078*, 421-443.
31. Shekaran, A.; Garcia, A. J., Nanoscale engineering of extracellular matrix-mimetic bioadhesive surfaces and implants for tissue engineering. *Biochimica et Biophysica Acta - General Subjects* **2011,** *1810*, 350-360.
32. Apte, G.; Hirtz, M.; Nguyen, T.-H., FluidFM-Based Fabrication of Nanopatterns: Promising Surfaces for Platelet Storage Application. *ACS Applied Materials & Interfaces* **2022,** *14*, 24133-24143.
33. Van Der Meer, P. F.; Kerkhoffs, J. L.; Curvers, J.; Scharenberg, J.; De Korte, D.; Brand, A.; De Wildt-Eggen, J., In vitro comparison of platelet storage in plasma and in four platelet additive solutions, and the effect of pathogen reduction: a proposal for an in vitro rating system. *Vox Sanguinis* **2010,** *98*, 517-524.
34. Berganza, E.; Apte, G.; Vasantham, S. K.; Nguyen, T.-H.; Hirtz, M., Integration of Biofunctional Molecules into 3D-Printed Polymeric Micro-/Nanostructures. *Polymers* **2022,** *14*, 1327.
35. Ventrici De Souza, J.; Liu, Y.; Wang, S.; Dörig, P.; Kuhl, T. L.; Frommer, J.; Liu, G. Y., Three-Dimensional Nanoprinting via Direct Delivery. *Journal of Physical Chemistry B* **2018,** *122*, 956-962.

CONTACTS

Dr. Thi Huong Nguyen email: thi-huong.nguyen@iba-heiligenstadt.de

ORCID: https://orcid.org/0000-0002-9237-3482

Author contributions: M.S. printed the structures, analyzed the data, discussed the results, and wrote the manuscript. A.G. performed platelet adhesion on the plastic bag. D.M. designed Pacman-like structures. T.H.N developed the study concept, discussed the results, performed the supervision, administered the project, acquired the funding, and wrote the manuscript. All authors have read and agreed to the final version of the manuscript.

Acknowledgments
We acknowledge the support of the Freistaat Thüringen (Thüringer Ministerium für Wirtschaft, Wissenschaft und Digitale Gesellschaft, TMWWDG, Germany) and the support of the German Research Foundation (DFG) within the projects (Nr. 469240103).

Conflicts of interest: The authors declare no conflict of interest.

